Microscopic Description of Intraband Absorption in Graphene: The Occurrence of Transient Negative Differential Transmission

Faris Kadi,[1,*] Torben Winzer,[1,2] Ermin Malic,[1] Andreas Knorr,[1] F. Göttfert,[3] M. Mittendorff,[3,4] S. Winnerl,[3] and M. Helm[3,4]

[1]*Institut für Theoretische Physik, Nichtlineare Optik und Quantenelektronik, Technische Universität Berlin,
Hardenbergstr. 36, 10623 Berlin, Germany*
[2]*Department of Materials Science and Engineering, Yonsei University, Seoul 120-749, Korea*
[3]*Helmholtz-Zentrum Dresden-Rossendorf, P.O. Box 510119, D-01314 Dresden, Germany*
[4]*Technische Universität Dresden, 01062 Dresden, Germany*
(Received 4 April 2014; published 16 July 2014)

We present a microscopic explanation of the controversially discussed transient negative differential transmission observed in degenerate optical pump-probe measurements in graphene. Our approach is based on the density matrix formalism allowing a time- and momentum-resolved study of carrier-light, carrier-carrier, and carrier-phonon interaction on microscopic footing. We show that phonon-assisted optical intraband transitions give rise to transient absorption in the optically excited hot carrier system counteracting pure absorption bleaching of interband transitions. While interband transition bleaching is relevant in the first hundreds of fs after the excitation, intraband absorption sets in at later times. In particular, in the low excitation regime, these intraband absorption processes prevail over the absorption bleaching resulting in a zero crossing of the differential transmission. Our findings are in good qualitative agreement with recent experimental pump-probe studies.

The ultrafast carrier relaxation dynamics in optically excited graphene has been intensively studied [1–12]. Typically, the carrier relaxation has been accessed via high-resolution pump-probe experiments [1,7,8,10,13]. Common to all studies is a biexponential decay of the pump-induced differential transmission (DT) spectrum expressing the ultrafast Coulomb-dominated carrier thermalization and the slower phonon-induced carrier cooling [7]. However, while some of the studies report on a purely positive transient DT spectrum [2,4,14], others exhibit a zero crossing after the initial decay [1,3,7,8,15–17]. The second decay component characterizes the recovering of the negative transient DT signal. There are a number of possible underlying mechanisms for the DT-zero crossing [1,3,7,8,11, 15–18]. For some of the experiments, the negative DT can be clearly traced back to the predominant intraband absorption. This is the case when the photon energy is smaller than twice the value of the Fermi energy [1,8,16]. However, for all other cases, where negative DT components occur for photon energies much larger than the Fermi energy, the underlying mechanism has been controversially discussed in literature. In particular, pump-induced band structure renormalization for transient [7] or in the long time limit [19] at the M point, as well as intraband absorption [9], have been suggested as explanations for the observed negative DT signals.

In this Letter, we present a microscopic explanation for the occurrence of transient negative DT in graphene. Based on the density matrix formalism, we investigate the detailed interplay of intra- and interband absorption processes on the transient DT in graphene. The absorptive electronic intraband transitions are assisted by emission or absorption of a phonon with an adequate momentum necessary to fulfill the momentum conservation, cf. Fig. 1. Intraband transitions are shown to lead to an enhanced absorption giving rise to the experimentally observed zero crossing from positive to negative DT signals. Existing studies taking into account intraband absorption based on the Kubo formalism [20] and the Drude model [9,21–23] are typically stationary and rely on phenomenological scattering rates. Our description goes significantly beyond these studies as we include time- and momentum-dependent phonon-assisted intraband absorption in a fully optical excited nonequilibrium situation on the same microscopic footing as the direct intra- and interband carrier-carrier and carrier-phonon scattering relaxation channels. In particular, we show that the parameter-free
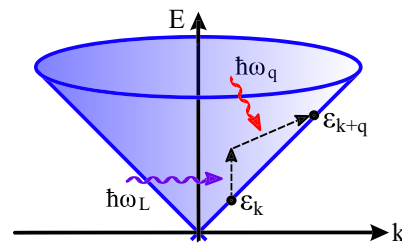

FIG. 1 (color online).   Illustration of the phonon-assisted intraband absorption within the linear band structure of graphene. Applying a pulse with the energy $\hbar\omega_L$ lifts electrons within the (conduction) band into an energetically higher electronic state. To conserve energy and momentum, this intraband absorption is assisted by an interaction with a phonon characterized by the energy $\hbar\omega_q$ and the momentum $\mathbf{q}$.

calculated transient ratio of inter- and intraband processes can explain many recent pump-probe experiments in graphene showing an interplay of positive and negative transmission.

The absorption coefficient $\alpha(\omega)$ of graphene is determined by the imaginary part of the optical susceptibility $\chi(\omega) = j(\omega)/[\epsilon_0 \omega^2 A(\omega)]$ with the current density $j(\omega)$, the vector potential $A(\omega)$, and the dielectric permittivity ϵ_0 [18]. The current reads

$$\mathbf{j}(t) = B \sum_{\mathbf{k}} \left[2\mathbf{M}_{\mathbf{k}}^{vc} \Im[p_{\mathbf{k}}] - i \sum_{\lambda} \left(\mathbf{M}_{\mathbf{k}}^{\lambda\lambda} \rho_{\mathbf{k}}^{\lambda} + \frac{e_0}{\hbar} \mathbf{A}(t) \rho_{\mathbf{k}}^{\lambda} \right) \right],$$

(1)

with the constant $B = 2e_0 \hbar/(m_0 L^2)$, where e_0 denotes the elementary charge, m_0 the free electron mass and L^2 the structure area that cancels out after performing the sum over $\mathbf{k}$. The current contains an interband (first term) and an intraband contribution (second and third terms). The coupling to the light is described by the interband or intraband optical matrix element $\mathbf{M}_{\mathbf{k}}^{\lambda\lambda'}$, respectively [24]. Furthermore, the current depends on the carrier occupation probability $\rho_{\mathbf{k}}^{\lambda}$ with the band index λ and the momentum $\mathbf{k}$ and the microscopic polarization $p_{\mathbf{k}}$ that is a measure for the optical transition probability [24]. These two microscopic quantities are determined by solving graphene Bloch equations [24]. It can be shown that the third term of the current $\mathbf{j}(t)$ in Eq. (1) cancels with the real part of the interband term resulting in a purely imaginary current [25]. Finally, the absorption coefficient can be written as

$$\alpha(\omega) = \frac{B}{\omega c_0 \epsilon_0} \sum_{\mathbf{k}} \Im \left[\frac{2M_{\mathbf{k}}^{vc} \Im[p_{\mathbf{k}}(\omega)]}{A(\omega)} - i \sum_{\lambda} \frac{M_{\mathbf{k}}^{\lambda\lambda} \rho_{\mathbf{k}}^{\lambda}(\omega)}{A(\omega)} \right],$$

(2)

where $M_{\mathbf{k}}^{\lambda\lambda'} = \mathbf{M}_{\mathbf{k}}^{\lambda\lambda'} \cdot \hat{\mathbf{e}}_{\mathbf{A}}$ with the direction of polarization of the vector potential $\hat{\mathbf{e}}_{\mathbf{A}}$. The interband contribution is proportional to $M_{\mathbf{k}}^{vc}$ and to the microscopic polarization $p_{\mathbf{k}}(\omega)$ leading to the well-known absorption spectrum of graphene with a constant value in the visible spectral range [18,26–30]. The phonon-assisted intraband processes influence the spectra via the carrier occupation probability $\rho_{\mathbf{k}}^{\lambda}(\omega)$ weighted by the optical intraband matrix element $\mathbf{M}_{\mathbf{k}}^{\lambda\lambda}$.

Since the main goal of our work is the description of the nonequilibrium regime, we focus on the DT spectrum that is determined by $\Delta T/T_0(\tau, \omega) \propto \alpha^{(t)}(\omega) - \alpha^{(p,t)}(\omega, \tau)$ with the absorption coefficient including both the pump and the probe (test) pulse $\alpha^{(p,t)}(\omega, \tau)$ and only the test pulse $\alpha^{(t)}(\omega)$ [31]. Assuming an isotropic carrier distribution in the momentum space after several fs [32], the transient DT reads

$$\Delta T/T_0(\tau, \omega)$$
$$\propto C_{k_\omega}[\Delta\rho_{k_\omega}^{(p,t)}(\tau) - \Delta\rho_{k_\omega}^{(t)}(\tau)]$$
$$+ \frac{i}{L^2 \omega A_0^{(t)}} \sum_{\lambda\mathbf{k}} M_{\mathbf{k}}^{\lambda\lambda} \Im[\rho_{\mathbf{k}}^{\lambda,(p,t)}(\omega, \tau) - \rho_{\mathbf{k}}^{\lambda,(t)}(\omega, \tau)], \quad (3)$$

with $C_{k_\omega} = |\mathbf{M}_{k_\omega}^{vc} \cdot \hat{\mathbf{e}}_{\mathbf{A}}|^2 e_0 \hbar^2/(8\pi m_0 v_F^2)$, $\Delta\rho_k = \rho_k^c - \rho_k^v$, the amplitude of the vector potential A_0, and the excitation momentum $k_\omega = \hbar\omega_L/2v_F$ with the pulse frequency ω_L and the carrier velocity close to the Dirac point v_F. The first line of Eq. (3) accounts for interband transitions, which reflects the absorption bleaching due to the additional carriers lifted from the valence into the conduction band by the pump pulse. As a result, the transient DT is expected to show a positive peak during the excitation. The second line describes the phonon-assisted intraband absorption processes that are induced by the probe pulse. Since these processes lead to an increased absorption after the excitation, we also expect a negative contribution to the transient DT signal.

To determine the interplay of these two contributions, we derive equations of motion for the carrier occupation probability $\rho_{\mathbf{k}}^{\lambda}$ and the microscopic polarization $p_{\mathbf{k}}$. To exploit the Heisenberg equation, we need the many-particle Hamilton operator H including the interaction-free carrier and phonon part H_0, the carrier-field coupling $H_{c,f}$, the carrier-phonon interaction $H_{c,p}$, and the carrier-carrier interaction $H_{c,c}$ [18,24]. In this Letter, we focus on the dynamics of the carrier occupation driven by the electron-phonon contribution $\dot{\rho}_{\mathbf{k}}^{\lambda}|_{H_{c,p}}$, which determines the phonon-assisted intraband absorption processes [33]. Other contributions can be found in Ref. [24]. Here, we discuss only the carrier-phonon interaction with $H_{c,p} = \sum_{\mathbf{l}_1 \mathbf{l}_2} \sum_{\mathbf{u}} (g_{\mathbf{u}}^{\mathbf{l}_1 \mathbf{l}_2} a_{\mathbf{l}_1}^{\dagger} a_{\mathbf{l}_2} b_{\mathbf{u}} + g_{\mathbf{u}}^{\mathbf{l}_1 \mathbf{l}_2 *} a_{\mathbf{l}_2}^{\dagger} a_{\mathbf{l}_1} b_{-\mathbf{u}}^{\dagger})$, where $a_{\mathbf{l}}^{\dagger}$ and $a_{\mathbf{l}}$ create and annihilate an electron in the state $\mathbf{l} = (\lambda, \mathbf{k})$, respectively. Furthermore, we introduce the bosonic operators $b_{\mathbf{u}}^{\dagger}$ and $b_{\mathbf{u}}$, which create and annihilate a phonon in the state $\mathbf{u} = (j, \mathbf{q})$ with the phonon momentum $\mathbf{q}$ and the different optical and acoustic phonon modes j. The strength of the carrier-phonon interaction is determined by the corresponding electron-phonon coupling elements $g_{\mathbf{u}}^{\mathbf{l}_1 \mathbf{l}_2}$ [34,35]. The phonon dispersion $\hbar\omega_{\mathbf{q}}^{j}$ is assumed to be constant for optical modes close to the Γ and K points [35] and linear for acoustic modes [34] close to the Γ point. Applying the Heisenberg equation of motion, we obtain

$$\dot{\rho}_{\mathbf{k}}^{\lambda}|_{H_{c,p}} = \frac{1}{i\hbar} \sum_{\lambda'} \sum_{j\mathbf{q}} (g_{\mathbf{k},\mathbf{q}}^{\lambda\lambda'j} S_{\mathbf{k},\mathbf{q}}^{\lambda\lambda'j} - g_{\mathbf{k}+\mathbf{q},\mathbf{q}}^{\lambda'\lambda j} S_{\mathbf{k}+\mathbf{q},\mathbf{q}}^{\lambda'\lambda j}$$
$$- g_{\mathbf{k},\mathbf{q}}^{\lambda\lambda'j*} T_{\mathbf{k},\mathbf{q}}^{\lambda'\lambda j} + g_{\mathbf{k}+\mathbf{q},\mathbf{q}}^{\lambda'\lambda j*} T_{\mathbf{k}+\mathbf{q},\mathbf{q}}^{\lambda\lambda'j}), \quad (4)$$

where $S_{\mathbf{k},\mathbf{q}}^{\lambda\lambda'j} = \langle a_{\mathbf{k}}^{\lambda\dagger} a_{\mathbf{k}-\mathbf{q}}^{\lambda'} b_{\mathbf{q}}^{j} \rangle$ and $T_{\mathbf{k},\mathbf{q}}^{\lambda\lambda'j} = \langle a_{\mathbf{k}-\mathbf{q}}^{\lambda\dagger} a_{\mathbf{k}}^{\lambda'} b_{\mathbf{q}}^{j\dagger} \rangle$ are phonon-assisted electron densities and transitions [36]. To obtain a closed system of differential equations, we derive additional equations for the phonon-assisted quantities [36,37]. Exemplary, we show the equation for $S_{\mathbf{k},\mathbf{q}}^{\lambda_1\lambda_2 j}$ reading

$$\dot{S}_{\mathbf{k},\mathbf{q}}^{\lambda_1\lambda_2 j} = \frac{i}{\hbar} \Delta\varepsilon_{\mathbf{k},\mathbf{q}}^{\lambda_1\lambda_2} S_{\mathbf{k},\mathbf{q}}^{\lambda_1\lambda_2 j} + \frac{i}{\hbar} \sum_{\lambda_3\lambda_4} g_{\mathbf{k},\mathbf{q}}^{\lambda_3\lambda_4 j*} Q_{\mathbf{k},\mathbf{q}}^{\lambda_1\lambda_3\lambda_4\lambda_2 j}$$
$$+ \frac{\hbar e_0}{m_0} \sum_{\lambda'} [S_{\mathbf{k},\mathbf{q}}^{\lambda_1\lambda'j} \mathbf{M}_{\mathbf{k}-\mathbf{q}}^{\lambda_2\lambda'} - S_{\mathbf{k},\mathbf{q}}^{\lambda'\lambda_2 j} \mathbf{M}_{\mathbf{k}}^{\lambda'\lambda_1}] \cdot \mathbf{A}(t), \quad (5)$$

with the energy $\Delta\varepsilon_{\mathbf{k},\mathbf{q}}^{\lambda_1\lambda_2} = \varepsilon_{\mathbf{k}}^{\lambda_1} - \varepsilon_{\mathbf{k}-\mathbf{q}}^{\lambda_2} - \hbar\omega_{\mathbf{q}}^j$ and the scattering kernel $Q_{\mathbf{k},\mathbf{q}}^{\lambda_1\lambda_2\lambda_3\lambda_4 j} = (\delta_{\lambda_1\lambda_2} - \sigma_{\mathbf{k}}^{\lambda_1\lambda_2})\sigma_{\mathbf{k}-\mathbf{q}}^{\lambda_3\lambda_4}n_{\mathbf{q}}^j - \sigma_{\mathbf{k}}^{\lambda_1\lambda_2}(\delta_{\lambda_3\lambda_4} - \sigma_{\mathbf{k}-\mathbf{q}}^{\lambda_3\lambda_4})(n_{\mathbf{q}}^j + 1)$, where $\sigma_{\mathbf{k}}^{\lambda\lambda'} = \langle a_{\mathbf{k}}^{\lambda\dagger}a_{\mathbf{k}}^{\lambda'}\rangle$ and $n_{\mathbf{q}}^j$ is the phonon occupation. The corresponding equation for $T_{\mathbf{k},\mathbf{q}}^{\lambda\lambda' j}$ can be derived in analogy [18,24].

The last term in Eq. (5) is of crucial interest for us, since it describes phonon-assisted optical transitions. They are driven by both carrier-light interaction ($\mathbf{M}_{\mathbf{k}}$) and also, implicitly, by carrier-phonon matrix elements appearing in the dynamics of the phonon-assisted quantity $S_{\mathbf{k},\mathbf{q}}^{\lambda_1\lambda_2 j}$. Our goal is the description of the phonon-assisted intraband absorption processes affecting the weak probe pulse applied after a much stronger pump pulse that creates a nonequilibrium carrier distribution. Since the experimentally observed negative transient DT spectrum occurs clearly after the application of the optical excitation, we study the interaction of the test pulse with the carrier occupation resulting from the pump-induced optical dynamics [7,11]. To be able to solve Eq. (5) analytically, we chose a perturbative approach assuming that $S_{\mathbf{k},\mathbf{q}}^{\lambda_1\lambda_2 j} = S_{\mathbf{k},\mathbf{q}(0)}^{\lambda_1\lambda_2 j} + \epsilon S_{\mathbf{k},\mathbf{q}(1)}^{\lambda_1\lambda_2 j}$ [33], where ϵ represents a small perturbation corresponding to the amplitude of the vector potential $\mathbf{A}_{\text{test}}(t) = \mathbf{A}_0 e^{-(t^2/2\sigma^2)}\cos(\omega_L t)$ describing the probe pulse with σ as the pulse duration. Within the well tested Markov approximation [24], the zeroth and the first order of $S_{\mathbf{k},\mathbf{q}}^{\lambda_1\lambda_2 j}$ are obtained analytically reading

$$S_{\mathbf{k},\mathbf{q}(0)}^{\lambda_1\lambda_2 j} = i\pi\sum_{\lambda_3\lambda_4} g_{\mathbf{k},\mathbf{q}}^{\lambda_3\lambda_4 j*} Q_{\mathbf{k},\mathbf{q}}^{\lambda_1\lambda_3\lambda_4\lambda_2 j} \delta(\Delta\varepsilon_{\mathbf{k},\mathbf{q}}^{\lambda_3\lambda_4}), \qquad (6)$$

$$S_{\mathbf{k},\mathbf{q}(1)}^{\lambda_1\lambda_2 j} = i\pi\sum_{\lambda_3\lambda_4} g_{\mathbf{k},\mathbf{q}}^{\lambda_3\lambda_4 j*} Q_{\mathbf{k},\mathbf{q}}^{\lambda_1\lambda_3\lambda_4\lambda_2 j} \frac{\frac{ie_0}{m_0}\Delta M_{\mathbf{k},\mathbf{q}}^{\lambda\lambda' j} e^{-\frac{t^2}{2\sigma^2}}}{2\Delta\varepsilon_{\mathbf{k},\mathbf{q}}^{\lambda_1\lambda_2}}$$
$$\times [e^{-i\omega_L t}\delta(\Delta\varepsilon_{\mathbf{k},\mathbf{q}}^{\lambda_3\lambda_4} + \hbar\omega_L)$$
$$+ e^{i\omega_L t}\delta(\Delta\varepsilon_{\mathbf{k},\mathbf{q}}^{\lambda_3\lambda_4} - \hbar\omega_L)], \qquad (7)$$

with $\Delta M_{\mathbf{k},\mathbf{q}}^{\lambda\lambda'} = (\mathbf{M}_{\mathbf{k}-\mathbf{q}}^{\lambda'\lambda'} - \mathbf{M}_{\mathbf{k}}^{\lambda\lambda})\cdot\hat{\mathbf{e}}_A$. All terms proportional to the off-diagonal matrix element $M_{\mathbf{k}}^{vc}$ turn out to cancel in the equation of $\rho_{\mathbf{k}}^{\lambda}$. The first order $S_{\mathbf{k},\mathbf{q}(1)}^{\lambda_1\lambda_2 j}$ describes the phonon-assisted intraband absorption, while the zeroth order $S_{\mathbf{k},\mathbf{q}(0)}^{\lambda_1\lambda_2 j}$ yields the standard Boltzmann-like equation containing phonon-assisted intra- and interband scattering processes.

Using Eqs. (6) and (7), the equation of motion for the carrier occupation $\rho_{\mathbf{k}}^{\lambda}$ can be written as

$$\dot{\rho}_{\mathbf{k}}^{\lambda}|_{H_{c,p}+H_{c,c}} = \tilde{\Gamma}_{\lambda,\mathbf{k}}^{\text{in}}(1 - \rho_{\mathbf{k}}^{\lambda}) - \tilde{\Gamma}_{\lambda,\mathbf{k}}^{\text{out}}\rho_{\mathbf{k}}^{\lambda}, \qquad (8)$$

with $\tilde{\Gamma}_{\lambda,\mathbf{k}}^{\text{in,out}} = \Gamma_{\lambda,\mathbf{k}}^{\text{in,out}} + \Gamma_{\lambda,\mathbf{k}}^{\text{in,out,A}}$. Here, $\Gamma_{\lambda,\mathbf{k}}^{\text{in,out}}$ describes the time- and momentum-dependent scattering rates including the Coulomb- and phonon-assisted contributions, which are discussed in detail in Ref. [24]. The field-assisted second order contribution $\Gamma_{\lambda,\mathbf{k}}^{\text{in,A}}$, responsible for the intraband absorption, reads

$$\Gamma_{\lambda,\mathbf{k}}^{\text{in,A}} = 2\pi\sum_{\lambda' jq}\left[|g_{\mathbf{k},\mathbf{q}}^{\lambda'\lambda j}|^2\left(\frac{\tilde{M}_{\mathbf{k},\mathbf{q}}^{\lambda'\lambda}}{\Delta\varepsilon_{\mathbf{k},\mathbf{q}}^{\lambda\lambda'}}\delta(\Delta\varepsilon_{\mathbf{k},\mathbf{q}}^{\lambda\lambda'}\pm\hbar\omega_L)\right)\rho_{\mathbf{k}-\mathbf{q}}^{\lambda'}n_{\mathbf{q}}^j\right.$$
$$\left.+ |g_{\mathbf{k}+\mathbf{q},\mathbf{q}}^{\lambda'\lambda j}|^2\left(\frac{\tilde{M}_{\mathbf{k}+\mathbf{q},\mathbf{q}}^{\lambda\lambda'}}{\Delta\varepsilon_{\mathbf{k}+\mathbf{q},\mathbf{q}}^{\lambda'\lambda}}\delta(\Delta\varepsilon_{\mathbf{k}+\mathbf{q},\mathbf{q}}^{\lambda'\lambda}\pm\hbar\omega_L)\right)\rho_{\mathbf{k}+\mathbf{q}}^{\lambda'}(n_{\mathbf{q}}^j+1)\right]$$
$$(9)$$

with $\tilde{M}_{\mathbf{k},\mathbf{q}}^{\lambda\lambda'} = ie_0/m_0(\mathbf{M}_{\mathbf{k}-\mathbf{q}}^{\lambda'\lambda'} - \mathbf{M}_{\mathbf{k}}^{\lambda\lambda})\cdot\mathbf{A}(t)$. It accounts for optically driven intraband absorption processes that are assisted by phonon absorption or emission fulfilling the momentum and energy conservation. The term $\Gamma_{\lambda,\mathbf{k}}^{\text{out,A}}$ can be obtained analogously by replacing $\rho \leftrightarrow \rho - 1$ and $n \leftrightarrow n + 1$. Basically, these terms have a similar form as the scattering rates $\Gamma_{\lambda,\mathbf{k}}^{\text{in,out}}$. Since they are proportional to the optical matrix elements $\tilde{M}_{\mathbf{k},\mathbf{q}}^{\lambda\lambda'}$, we expect them to have a contribution to the DT.

Similar to Eq. (5), Eq. (8) can be further simplified by using the ansatz $\rho_{\mathbf{k}}^{\lambda}(t) = \rho_{\mathbf{k}}^{\lambda,0}(t) + \delta\rho_{\mathbf{k}}^{\lambda}(t)$. Here, $\rho_{\mathbf{k}}^{\lambda,0}(t)$ contains the pump-induced occupation resulting from the Coulomb- and phonon-assisted scattering rates $\Gamma_{\lambda,\mathbf{k}}^{\text{in,out}}$ [18], while $\delta\rho_{\mathbf{k}}^{\lambda}(t)$ describes a small perturbation induced by the probe pulse. The latter, in particular, is driven by phonon-assisted intraband absorption processes. Assuming a weak δ-shaped probe pulse $\mathbf{A} = \mathbf{A}_0\delta(t - \tau)$, the Fourier transform for the perturbation yields

$$\delta\rho_{\mathbf{k}}^{\lambda}(\omega,\tau) = \frac{\Gamma_{\lambda,\mathbf{k}}^{\text{in,A}}(1 - \rho_{\mathbf{k}}^{\lambda,0}(\tau)) - \Gamma_{\lambda,\mathbf{k}}^{\text{out,A}}\rho_{\mathbf{k}}^{\lambda,0}(\tau)}{i\omega + \tilde{\gamma}}, \qquad (10)$$

where the small damping $\tilde{\gamma} = \Gamma_{\lambda,\mathbf{k}}^{\text{in}} + \Gamma_{\lambda,\mathbf{k}}^{\text{out}}$ is assumed to be constant. In the expression of $\delta\rho_{\mathbf{k}}^{\lambda}(\omega,\tau)$, we neglect the nonlinear terms proportional to $\mathbf{A}(t)$, assuming a weak probe pulse.

Inserting Eq. (10) into Eq. (3), we can evaluate the impact of phonon-assisted intraband absorption processes on the transient DT. First, we analyze the impact of the excitation strength on the transient DT spectrum. Figure 2 shows the calculated degenerate transient DT spectrum $\Delta T/T_0(\tau)$ excited by a 50 fs pulse with a pump fluence of $8\ \mu J/\text{cm}^2$ at the photon energy $E = 1.5$ eV. The abrupt increase of the signal reflects the ultrafast optical injection of nonequilibrium carriers around the photon energy resulting in an absorption bleaching. Afterwards, the signal decreases on a fs time scale due to the carrier-carrier and carrier-phonon scattering [7]. Taking into account only interband absorption (Fig. 2, thin line), the transient DT signal remains positive during the entire dynamics. However, after including the phonon-assisted intraband absorption, the transient exhibits a distinct zero-crossing after approximately 310 fs followed by a subsequent recovery towards zero on a ps time scale. This observation reflects well the experimental observation, as will be discussed below.

For both theory curves in Fig. 2, we find a biexponential decay characterized by a fast time constant $\tau_1 = 90$ fs and a
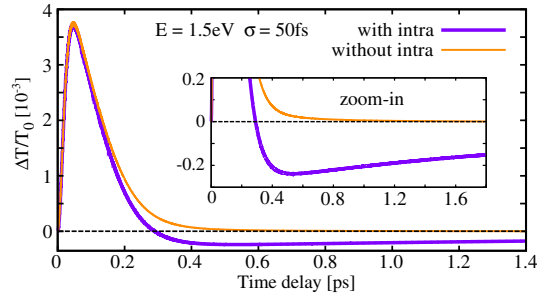
FIG. 2 (color online).   Transient differential transmission spectrum as a function of the delay time τ between the pump and the probe pulse illustrating the impact of phonon-assisted intraband processes, which account for a zero crossing.

slow component $\tau_2^{\text{inter}} = 0.6$ ps (positive DT, thin orange line) and $\tau_2^{\text{inter+intra}} = 2.8$ ps (negative DT, thick violet line) depending on whether intraband processes are included or not. The intraband absorption does not change the first decay rate; however, the second decay is considerably slowed down in the presence of intraband absorption. The decay τ_2^{inter} is determined by the electron cooling due to electron-phonon interaction, whereas the decay $\tau_2^{\text{inter+intra}}$ in the presence of intraband absorption has a different origin: Since intraband absorption always occurs for a finite carrier population, $\tau_2^{\text{inter+intra}}$ is limited by carrier recombination processes that take place on a slower time scale (several ps) than the carrier cooling (one ps).

Figure 3(a) illustrates the impact of the phonon-assisted intraband absorption on the transient DT at different pump fluences covering the range of 2–24 $\mu J/\text{cm}^2$. The fast decay time τ_1 exhibits a weak increase from 80 to 110 fs with the increasing fluence. In the case of weak excitation, the thermalized carrier distribution differs only slightly from the initial thermal distribution. Because of the low population, the impact of Pauli blocking above the thermal tail is almost negligible with the consequence that the out scattering from the excited states becomes very efficient and leads to a fast decay τ_1. For stronger excitation, the efficient Pauli blocking suppresses the out scattering explaining the increased τ_1 time [38]. In contrast to the fast decay component, the slower τ_2 time decreases approximately linearly from 3.3 to 2.7 ps with increasing pump fluence: At high excitation, there is an increased number of excited carriers at the Dirac point resulting in faster recombination of the carrier system.

To test the predicted behavior, we compare our results with recently performed experimental data [11] depicted in Fig. 3(b). Investigating increasing pump intensity, we find, both in theory and experiment, (i) similar time scales τ, (ii) the same trend of the zero-crossing, and (iii) height trend as a function of pump intensity. The absolute value of the negative transient DT signal increases with the pump fluence, compare the insets of Figs. 3(a) and 3(b). At high fluences, the intraband absorption is enhanced due to the larger number of available carriers in the conduction band. At the same time, increasing
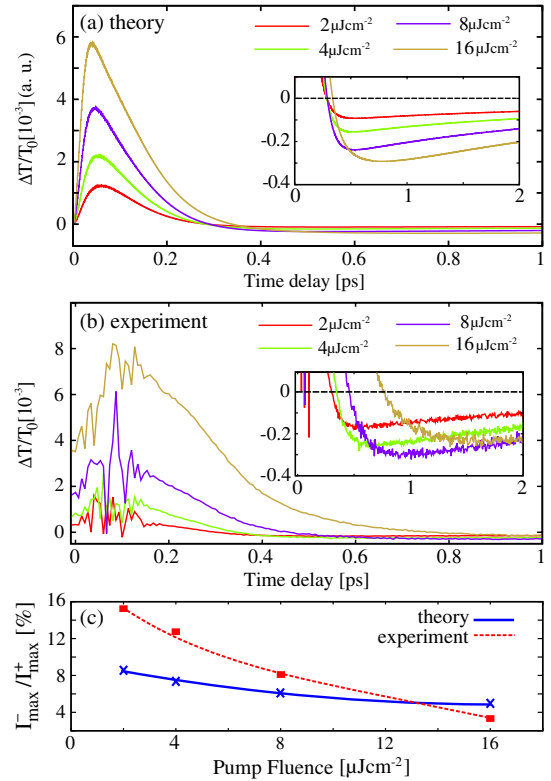

FIG. 3 (color online).   (a) Transient differential transmission spectrum for different pump fluences including the phonon-assisted intraband absorption processes. (b) Experimentally measured transient differential transmission at the same conditions (excitation energy of 1.5 eV and a pulse width of 50 fs). (c) Fluence-dependent ratio $I^-_{\text{max}}/I^+_{\text{max}}$ denoting the maximal negative and positive transient DT signal, respectively. The strongest relative impact of phonon-assisted intraband processes is predicted at small fluences —in good agreement with the experiment.

the fluence gives rise to a more efficient Pauli blocking, which increases the absorption bleaching and leads to a stronger positive DT signal. Figure 3(c) shows the fluence dependence of the ratio $I^-_{\text{max}}/I^+_{\text{max}}$ between the maximal negative (I^-_{max}) and positive (I^+_{max}) transient DT signal. The maxima have been extracted from the experimental data by performing a fitting that takes into account the shape of the laser pulse and the exponential decay with different time constants. We find a good qualitative agreement between the theoretically predicted and experimentally measured behaviors: The ratio clearly decreases with the fluence with a maximal ratio in the range of 10% found in the weak excitation regime. The decrease can be traced back to the predominant role of the Pauli blocking at high fluences prevailing over the increased efficiency of intraband absorption. This also explains the observation both in theory and experiment that the zero crossing occurs at larger delay times with the increasing fluence, cf. the insets of Figs. 3(a) and 3(b). The theoretically predicted values for τ_2 correspond well with the time scale experimentally observed.

The focus of our work lies on a qualitative understanding of the negative DT based on a microscopic theory without

adjustable parameters. The appearing quantitative deviations might be due to the neglected effects of Coulomb-induced intraband absorption processes and energy renormalization as well as due to the influence of substrate-induced doping and sample impurities. In particular, the Coulomb-assisted processes are expected to become important in the high excitation regime and could explain the more pronounced fluence dependence of the temporal zero crossing in the experimental DT spectrum.

In conclusion, we propose a microscopic mechanism explaining the occurrence of the transient negative differential transmission in graphene that has been observed in several recent pump-probe experiments. Our calculations reveal that the interplay of interband and phonon-assisted intraband absorption processes provides a qualitative explanation of this effect: phonon-induced processes open an additional absorption channel assisted by simultaneous absorption or emission of phonons that are required to fulfill the conservation of momentum.

---

[*]faris.kadi@mailbox.tu-berlin.de

[1] D. Sun, Z.-K. Wu, C. Divin, X. Li, C. Berger, W. A. de Heer, P. N. First, and T. B. Norris, Phys. Rev. Lett. **101**, 157402 (2008).

[2] J. M. Dawlaty, S. Shivaraman, M. Chandrashekhar, F. Rana, and M. G. Spencer, Appl. Phys. Lett. **92**, 042116 (2008).

[3] P. Plochocka, P. Kossacki, A. Golnik, T. Kazimierczuk, C. Berger, W. A. de Heer, and M. Potemski, Phys. Rev. B **80**, 245415 (2009).

[4] H. Wang, J. H. Strait, P. A. George, S. Shivaraman, V. B. Shields, M. Chandrashekhar, J. Hwang, F. Rana, M. G. Spencer, C. S. Ruiz-Vargas, and J. Park, Appl. Phys. Lett. **96**, 081917 (2010).

[5] X. Zou, D. Zhan, X. Fan, D. Lee, S. K. Nair, L. Sun, Z. Ni, Z. Luo, L. Liu, T. Yu, Z. Shen, and E. E. M. Chia, Appl. Phys. Lett. **97**, 141910 (2010).

[6] F. Wendler, A. Knorr, and E. Malic, Nat. Commun. **5**, 3703 (2014).

[7] M. Breusing, S. Kuehn, T. Winzer, E. Malić, F. Milde, N. Severin, J. P. Rabe, C. Ropers, A. Knorr, and T. Elsaesser, Phys. Rev. B **83**, 153410 (2011).

[8] S. Winnerl, M. Orlita, P. Plochocka, P. Kossacki, M. Potemski, T. Winzer, E. Malic, A. Knorr, M. Sprinkle, C. Berger, W. A. de Heer, H. Schneider, and M. Helm, Phys. Rev. Lett. **107**, 237401 (2011).

[9] L. M. Malard, K. F. Mak, A. H. C. Neto, N. M. R. Peres, and T. F. Heinz, New J. Phys. **15**, 015009 (2013).

[10] P. A. Obraztsov, M. G. Rybin, A. V. Tyurnina, S. V. Garnov, E. D. Obraztsova, A. N. Obraztsov, and Y. P. Svirko, Nano Lett. **11**, 1540 (2011).

[11] S. Winnerl, F. Göttfert, M. Mittendorff, H. Schneider, M. Helm, T. Winzer, E. Malic, A. Knorr, M. Orlita, M. Potemski, M. Sprinkle, C. Berger, and W. A. d. Heer, J. Phys. Condens. Matter **25**, 054202 (2013).

[12] T. Winzer, A. Knorr, M. Mittendorff, S. Winnerl, M.-B. Lien, D. Sun, T. B. Norris, M. Helm, and E. Malic, Appl. Phys. Lett. **101**, 221115 (2012).

[13] J. H. Strait, H. Wang, S. Shivaraman, V. Shields, M. Spencer, and F. Rana, Nano Lett. **11**, 4902 (2011).

[14] S. Kumar, M. Anija, N. Kamaraju, K. S. Vasu, K. S. Subrahmanyam, A. K. Sood, and C. N. R. Rao, Appl. Phys. Lett. **95**, 191911 (2009).

[15] R. W. Newson, J. Dean, B. Schmidt, and H. M. van Driel, Opt. Express **17**, 2326 (2009).

[16] D. Sun, C. Divin, C. Berger, W. A. de Heer, P. N. First, and T. B. Norris, Phys. Rev. Lett. **104**, 136802 (2010).

[17] J. Shang, Z. Luo, C. Cong, J. Lin, T. Yu, and G. G. Gurzadyan, Appl. Phys. Lett. **97**, 163103 (2010).

[18] E. Malic and A. Knorr, *Graphene and Carbon Nanotubes: Ultrafast Optics and Relaxation Dynamics* (Wiley, New York, 2013), 1st ed.

[19] A. T. Roberts, R. Binder, N. H. Kwong, D. Golla, D. Cormode, B. J. Leroy, H. O. Everitt, and A. Sandhu, Phys. Rev. Lett. **112**, 187401 (2014).

[20] B. Y. Sun and M. W. Wu, Phys. Rev. B **88**, 235422 (2013).

[21] H. Choi, F. Borondics, D. A. Siegel, S. Y. Zhou, M. C. Martin, A. Lanzara, and R. A. Kaindl, Appl. Phys. Lett. **94**, 172102 (2009).

[22] S. A. Mikhailov and K. Ziegler, Phys. Rev. Lett. **99**, 016803 (2007).

[23] L. A. Falkovsky and S. S. Pershoguba, Phys. Rev. B **76**, 153410 (2007).

[24] E. Malic, T. Winzer, E. Bobkin, and A. Knorr, Phys. Rev. B **84**, 205406 (2011).

[25] J. E. Sipe and E. Ghahramani, Phys. Rev. B **48**, 11705 (1993).

[26] K. F. Mak, J. Shan, and T. F. Heinz, Phys. Rev. Lett. **106**, 046401 (2011).

[27] T. Stauber, N. M. R. Peres, and A. K. Geim, Phys. Rev. B **78**, 085432 (2008).

[28] R. R. Nair, P. Blake, A. N. Grigorenko, K. S. Novoselov, T. J. Booth, T. Stauber, N. M. R. Peres, and A. K. Geim, Science **320**, 1308 (2008).

[29] K. F. Mak, M. Y. Sfeir, Y. Wu, C. H. Lui, J. A. Misewich, and T. F. Heinz, Phys. Rev. Lett. **101**, 196405 (2008).

[30] A. K. Geim and K. S. Novoselov, Nat. Mater. **6**, 183 (2007).

[31] S. Mukamel, *Principles of Nonlinear Optical Spectroscopy* (Oxford University Press, New York, 1999).

[32] E. Malic, T. Winzer, and A. Knorr, Appl. Phys. Lett. **101**, 213110 (2012).

[33] M. Kira, W. Hoyer, and S. W. Koch, Phys. Status Solidi B **238**, 443 (2003).

[34] E. H. Hwang and S. Das Sarma, Phys. Rev. B **77**, 115449 (2008).

[35] S. Piscanec, M. Lazzeri, F. Mauri, A. C. Ferrari, and J. Robertson, Phys. Rev. Lett. **93**, 185503 (2004).

[36] J. Schilp, T. Kuhn, and G. Mahler, Phys. Rev. B **50**, 5435 (1994).

[37] F. Rossi, S. Haas, and T. Kuhn, Phys. Rev. Lett. **72**, 152 (1994).

[38] T. Winzer and E. Malic, J. Phys. Condens. Matter **25**, 054201 (2013).